Materials and Design 195 (2020) 108930

Contents lists available at ScienceDirect

Materials and Design

journal homepage: www.elsevier.com/locate/matdes

3D printed origami honeycombs with tailored out-of-plane energy absorption behavior

Scott Townsend *, Rhosslyn Adams, Michael Robinson, Benjamin Hanna, Peter Theobald

School of Engineering, Cardiff University, Cardiff, UK

HIGHLIGHTS

- A method was developed to introduce origami fold patterns into square honeycombs.
- The origami honeycombs were realized via 3D printing in thermoplastic polyurethane.
- The crushing behavior of the origami honeycombs was studied via finite element analysis and experimental compression testing.
- Varying the origami fold parameters allows significant tailoring of the honeycomb stress-strain response.
- Absorption efficiencies as high as 0.49 were experimentally demonstrated, which rivals that of rigid polyurethane foams.

GRAPHICAL ABSTRACT

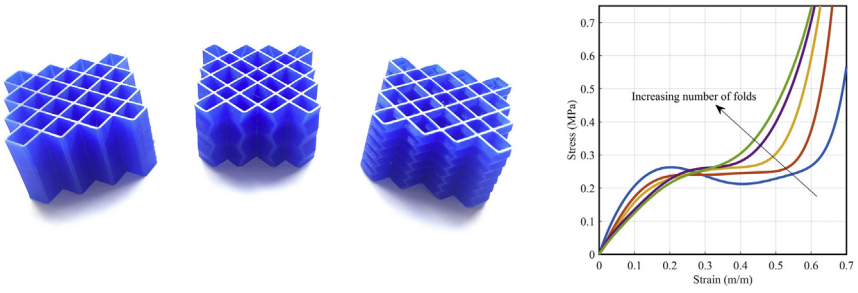

ARTICLE INFO

Article history:
Received 13 May 2020
Received in revised form 23 June 2020
Accepted 25 June 2020
Available online 10 July 2020

Keywords:
3D printing
Origami
Honeycomb
Out-of-plane
Post-buckling

ABSTRACT

Honeycomb structures display extraordinary stiffness-to-weight ratio when loaded in the out-of-plane direction. When realized using thermoplastic polyurethane (TPU), the structures offer the potential for repeatable and high specific energy absorption. Varying the cell size and wall thickness of TPU honeycombs facilitates changes in stiffness magnitude, though affords only modest capacity to alter the shape of the stress-strain curve. 3D printing facilitates advanced design exploration, beyond that of straight walls. Origami fold patterns have demonstrated the ability to influence the buckling behavior of tubular structures. Here we demonstrate the incorporation of origami folds into square honeycombs. The fold parameters facilitate significant tailoring of the stress-strain curve, allowing a range of profiles from quasi-rectangular to quasi-linear to be achieved; such structures can find applications in situation-specific energy absorption scenarios.

1. Introduction

Cellular structures (foams, lattices, honeycombs) can be designed to undergo large compressive strains at near-constant stress, making them ideal energy absorbers [1]. The remarkable stiffness-to-weight ratio of honeycombs loaded in the out-of-plane (or axial) direction has inspired particular research interest, and found countless applications in aerospace, transportation, building construction and sporting equipment [2].

Depending on the base material and loading conditions, honeycomb structures can undergo large out-of-plane compressive deformation via elastic buckling, plastic collapse or brittle failure [1]. Single-use energy absorbers, comprised for example of metal [3] or paper [4], have long

* Corresponding author.
E-mail address: townsends3@cf.ac.uk (S. Townsend).

https://doi.org/10.1016/j.matdes.2020.108930

attracted research attention. There is now renewed interest in the design of repeatable impact materials, particularly in applications of human safety such as fall cushioning [5] and concussion prevention [6]. As a route to repeatability, researchers have investigated using the shape recovery effect in honeycombs comprised of polycaprolactone [7] and polypropylene-like [8] materials. Despite largely recovering their original shape, these structures were observed to retain significant plastic damage, with a large discrepancy in stiffness between the first and subsequent compression cycles. Thermoplastic polyurethane (TPU) presents an alternative route, can be manufactured in a wide array of stiffness and is known for its excellent impact properties, capable of undergoing large elastically-recoverable strains, making it well-suited to repeated impact scenarios [9]. While basic honeycomb structures comprising straight walls at constant thickness may be cast or injection molded, TPU can also be manufactured via selective laser sintering (SLS) and fused filament fabrication (FFF) 3D printing, facilitating the exploration of additional honeycomb design variables.

Hexagonal TPU honeycombs with straight walls at constant thickness have been 3D printed and studied under in-plane compression [10]. The specific energy absorption was tuned via the relative density parameter (proportional to the ratio of wall thickness to length). These structures demonstrated energy absorbing efficiencies comparable to that of polyurethane foams, and were shown to recover after being subjected to multiple compressive cycles to densification. The flexibility of 3D printing allowed the extension of this work to include in-plane relative density grading, which effected significant modification of the energy absorption profile [11]. The out-of-plane compression behavior of 3D printed TPU honeycombs was demonstrated in [12]. The response was typical of honeycombs comprised of other materials, namely displaying an initial high peak stress, followed by a relatively-flat plateau prior to densification [13]. Such a response typically results in low energy absorption efficiency, as the initial peak absorbs little energy, though incurs very high stress levels. To the authors' knowledge, there are no studies to date specifically-focused on the design of 3D printed TPU honeycombs for tailored out-of-plane behavior; such is the focus of the present work.

The above notwithstanding, a number of design approaches have proven effective in modifying energy absorption in structures other than TPU honeycombs, for example the use of variable-thickness cell edges [14], tube reinforcement in thin walls [15] and hierarchical design [16]. A design strategy garnering particular research attention is the introduction of origami folds in axially-compressed structures. The presence of fold patterns can guide the crushing mode, remove the initial peak stress and reduce fluctuations in the plateau region. This has been demonstrated for metallic tubes incorporating several types of fold patterns, including diamond [17] and Miura-Ori [18] shapes. In Ref. [19], a fold pattern was implemented which, for square tubes, approximates the natural "symmetric" crushing mode of a straight-walled tube [20], thus providing a theoretical grounding for the design modification in guiding the crush mode. The same crushing mode is present in square honeycombs [21], suggesting the same fold pattern could be utilized in tailoring square honeycomb out-of-plane behavior. In this way, it becomes feasible to retain the stiffness-to-weight ratio of axially-compressed honeycombs, though remove the undesirable, inefficient peak stress prevalent in straight-walled designs.

In this article we demonstrate the effect of including origami fold patterns on the energy absorption behavior of 3D printed square TPU honeycombs. By tuning the geometric parameters, we achieve energy absorption profiles ranging from quasi-rectangular to quasi-linear. Section 2 describes the structural geometry and tuning parameters. Section 3 details the 3D printing fabrication procedures. Section 4 presents the experimental compression results. Conclusions and outlook are provided in Section 5.

2. Geometry

The square origami honeycomb comprises an array of square tubes, each of which incorporates the fold pattern. The geometry of a single square tube depicted in Fig. 1a and c is described by five parameters: wall thickness t, cell width w and aspect ratio $e \in (0,1]$ comprise the in-plane parameters, while height h and number of folds n comprise the out-of-plane parameters. Note that an aspect ratio $e = 1$ retrieves a tube with a square cross-section, and thus straight walls in the z-direction; as e reduces, the cross-section of the tube becomes more rectangular, and consequently the fold angles become more severe. As such, e simultaneously-controls the ratio of side lengths in the cross section, and the fold angles in the z-direction. By inspection, the extreme x and y edges are straight; the single tube can thus be successively mirrored in the x and y directions to form a fully connected honeycomb tiling. A 4×4 example is depicted in Fig. 1b and d with $t = 1$ mm, $w = 12.5$ mm, $e = 0.6$, $h = 30$ mm and $n = 4$.

By inspection of the geometry in Fig. 1a, a given cross-section comprises a rectangle with side lengths $l_1 = \sqrt{2}\frac{w}{1+e}$, $l_2 = \sqrt{2}(w - l_1)$, wall thickness t and corners removed. The area of said rectangle is thus equal to $A = 2t(l_1 + l_2) - 4\left(\frac{t^2}{2}\right) = 2\sqrt{2}tw - 2t^2$, where the second term accounts for the squared-off corners. Since the cross section area

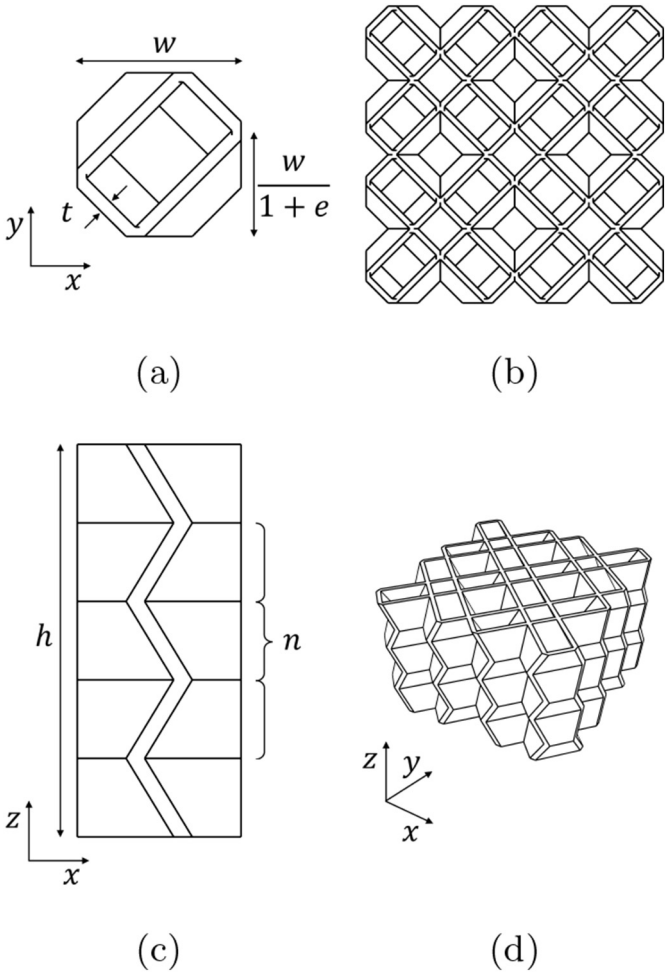

Fig. 1. Geometry of the square origami honeycomb. The patterned square tube (a), (c) is successively mirrored in the x and y directions to form a fully-connected honeycomb tiling (b), (d).

is independent of height, the volume of a tube is simply Ah. The relative density of a given tube is thus equal to:

$$\rho_{rel} = \frac{Ah}{w^2 h} = \frac{2\sqrt{2}t}{w} - 2\left(\frac{t}{w}\right)^2 \quad (1)$$

The volume of material in (and thus weight of) an origami honeycomb thus depends only on w, h and t, and not on e or n.

In order to visualize the out-of-plane compression behavior of square TPU origami honeycombs, several exemplary designs were subjected to finite element analysis (FEA) using ABAQUS 2019 (Dassault Systems, France). The TPU selected as the base material was Ninjaflex (Ninjatek, USA), for which an ABAQUS material card has been developed previously [12]. Briefly, a Mooney-Rivlin hyperelastic material model is used, calibrated using uniaxial, equi-biaxial and planar test data on 3Dprinted coupons. The hyperelastic constants used were $C_{10} = 2.930$ MPa, $C_{01} = 0.363$ MPa, $D_1 = 0.0$. The friction coefficient was estimated as 1.0. Full details of the material characterization can be found in Ref [12]. Although we herein focus on the quasi-static structural response, the explicit dynamic solver in ABAQUS was utilized in order to access the general contact algorithm. The deformation speed was set to 1.0 m/s, with no viscoelastic effects considered. Mesh generation was undertaken using an in-house meshing program, and for each geometry, mesh size was selected to be half that of the wall thickness. Numerical experiments confirmed that reducing the deformation speed and mesh size produced negligible changes in the structural behavior discussed below.

The FEA results are shown in Fig. 2. The straight-walled square honeycomb with $e = 1.0$ produces a stress-strain curve with a high initial peak stress, followed by a significant drop prior to the plateau region and densification. This behavior corresponds to the structure initially following a symmetric crushing mode [21] shown in Fig. 2c and d, though at higher strains undergoing a secondary collapse as shown in Fig. 2e. By inspection of Fig. 2d, the symmetric crushing mode naturally has 4 fold lines. We thus maintained $n = 4$ in the two subsequent designs, though reduced the aspect ratio to $e = 0.8$ and $e = 0.6$ respectively. The stress-strain response of the $e = 0.8$ design displays a reduced initial stiffness, lower peak stress and a less-significant drop between the peak and plateau stress values. Accordingly, only remnants of the secondary collapse mode remain in Fig. 2h and i. The $e = 0.6$ design has further-reduced the initial stiffness, and all but removed the difference between peak and plateau stress. As shown in Fig. 2k–m the $e = 0.6$ structure remains guided on the symmetric crush mode even at very high compressive strains.

3. Fabrication by 3D printing

The origami honeycombs were manufactured via FFF 3D printer (2017 Flashforge Creator Pro), retrofitted with high-specification extrusion control (Diabase Engineering, USA). As noted above, the filament was Ninjaflex (Ninjatek, USA), a commercially-available TPU, with nominal density 1190 kg/m^3. STL files were generated using the in-house meshing program noted above. Simplify3D (Simplify3D, USA) was used to define print settings and slice the STL files for printing. The printer settings were previously-optimized for part quality assessed via micro-CT. Briefly, the nozzle diameter was 0.4 mm, print speed 2000 mm/min, bed temperature 40°C, extruder temperature 210°C, layer height 0.1 mm. Full details regarding the selection of the printer parameters can be found in Ref. [12]. Each manufactured design had nominal wall thickness $t = 1.0$ mm, cell width $w = 12.5$ mm, and height $h = 30.0$ mm, while aspect ratio e and number of folds n was varied. Fig. 3 depicts three examples of the 3D printed structures. In all, nine designs were manufactured. As per Eq. 1, each design had a nominal relative density of 0.21, which amounts to a mass of 19.1 g. For reference, these values were chosen as they are considered especially-relevant to American football helmet applications. Namely, $h = 30.0$ mm is representative of the thickness of most helmet padding layers, and the chosen combination of t and w results in designs with stress plateaus on the order of 0.25 MPa, similar to the elastomeric foams used in commercial football helmets.

4. Experimental results

Experimental compression tests were performed using an electromechanical uniaxial testing machine (Zwick Z50, Germany) at a rate of 100 mm/min. The TPU origami honeycomb is expected to find application in personal protective equipment, such as football helmets and safety flooring. Thus, the low-friction steel contacts of the uniaxial testing machine are not considered representative of real-world boundary conditions, where friction effects would be more significant. Namely, the TPU is likely to contact skin, plastic, or other elastomeric surfaces. Sheets of 1 mm thick Ninjaflex were thus taped to the upper and lower compression surfaces to simulate a nominal frictional contact condition. As noted above, each specimen had the same cell width, wall thickness and height, while the aspect ratio e and number of folds n were varied. As such, we investigated the relationship between origami parameters e,n and the energy absorption behavior of the honeycomb. Three specimens of each design were tested, though no significant variation in behavior was observed. This is considered a result of the extensive print calibration done in a previous study [12]. The results which follow are for one specimen of each design. Strain was calculated by dividing the deflection of the uniaxial testing machine by the honeycomb height h. Stress was calculated by dividing the recorded force by the projected area of the samples, i.e. $(4w)^2 = 2500$ mm^2. Fig. 4a depicts the stress-strain response of the origami honeycomb for varying aspect ratio e with constant number of folds $n = 6$. As predicted by the FEA results above, the straight-walled honeycomb (with $e = 1.0$) displays a high peak stress, followed by a secondary collapse and plateau prior to densification. As e decreases, the difference between peak and plateau stress diminishes. For $e \leq 0.9$, a quasi-rectangular response is observed, which as per the previous FEA results corresponds to the structure being guided sufficiently and remaining in the symmetric crush mode for all strains. Also evident is a significant reduction in overall stiffness as e is reduced: the plateau stress approximately halves by reducing e from 0.9 to 0.6. The densification strain, however, largely remains unchanged, with all designs densifying between approximately 0.55 and 0.60 m/m strain.

In order to facilitate comparison with previous studies [10,22], we also plotted in Fig. 4b the efficiency parameter, defined as [23]:

$$\text{Efficiency}(\varepsilon) = \frac{1}{\sigma_{max}} \int_0^{\varepsilon} \sigma(\varepsilon) \cdot d\varepsilon \quad (2)$$

where σ_{max} is defined as the maximum stress up to the given strain ε. Accordingly, the efficiency parameter measures the ratio between the energy absorbed by a structure when compressed to a given strain and that absorbed by an ideal foam which transmits the constant stress σ_{max} at all strains and when fully-compressed. Note that while efficiency is defined relative to strain, it is typically plotted in the literature against the corresponding stress recorded at a given strain, as in Fig. 4b. The 3D printed Ninjaflex honeycombs studied in Ref. [10], which were compressed in the transverse direction, recorded maximum efficiencies of 0.37, while the rigid foams studied in Ref. [22] recorded values as high as 0.50.

As per Fig. 4a and b, the stress which gives maximum absorption efficiency, denoted by dots on the corresponding curves, reduces with e. The maximum efficiency parameter value, however, shows only minor variation, with values ranging between 0.42 and 0.46 for all structures excluding the straight-walled honeycomb. This is due to all designs other than the straight-walled design having a quasi-rectangular shape and similar densification strain, with plateau stress value

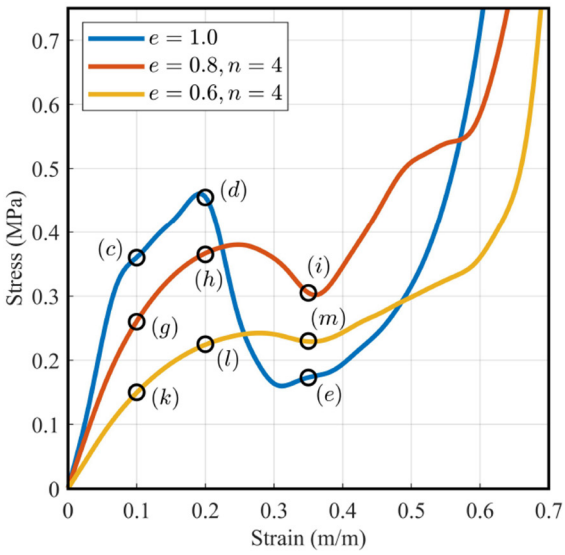

(a) Stress-strain curves. Inset labels correspond to deformation states below.

Fig. 2. Finite element analysis of three Ninjaflex TPU origami honeycombs under quasi-static compression. For each, $w = 12.5$ mm, $t = 1.0$ mm, $h = 30.0$ mm. (b)–(e), (f)–(i) and (j)–(m) depict the deformation for the $e = 1.0$, $e = 0.8$ and $e = 0.6$ designs respectively.

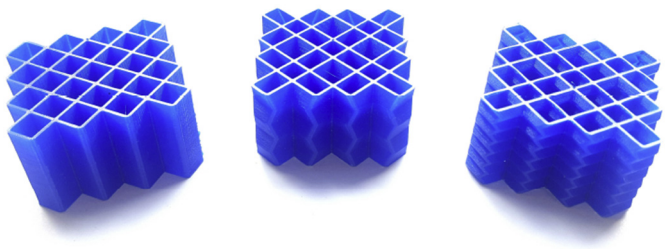

Fig. 3. FFF printed origami honeycombs. Specimens shown have $t = 1.0$ mm, $w = 12.5$ mm, $h = 30.0$ mm and $e = 1.0$ (left), $e = 0.7$, $n = 6$ (center), $e = 0.7$, $n = 12$ (right).

reducing with e. The straight-walled honeycomb records a reduced maximum efficiency of 0.38.

Fig. 5a depicts results for varying number of folds n with constant aspect ratio $e = 0.7$. Remnants of a secondary collapse are evident for the $e = 0.7$, $n = 4$ design, however as n increases, the response transitions from quasi-rectangular to quasi-linear. As per Fig. 5b, the stress at which maximum absorption efficiency occurs increases only marginally with increasing n, however the efficiency values reduce substantially, from a maximum value of 0.49 at $n = 4$ to 0.25 at $n = 12$.

Based on the above observations, the effect of e and n can be interpreted as follows: given a general energy absorption curve comprised of three regions – initial linear slope, plateau and densification,

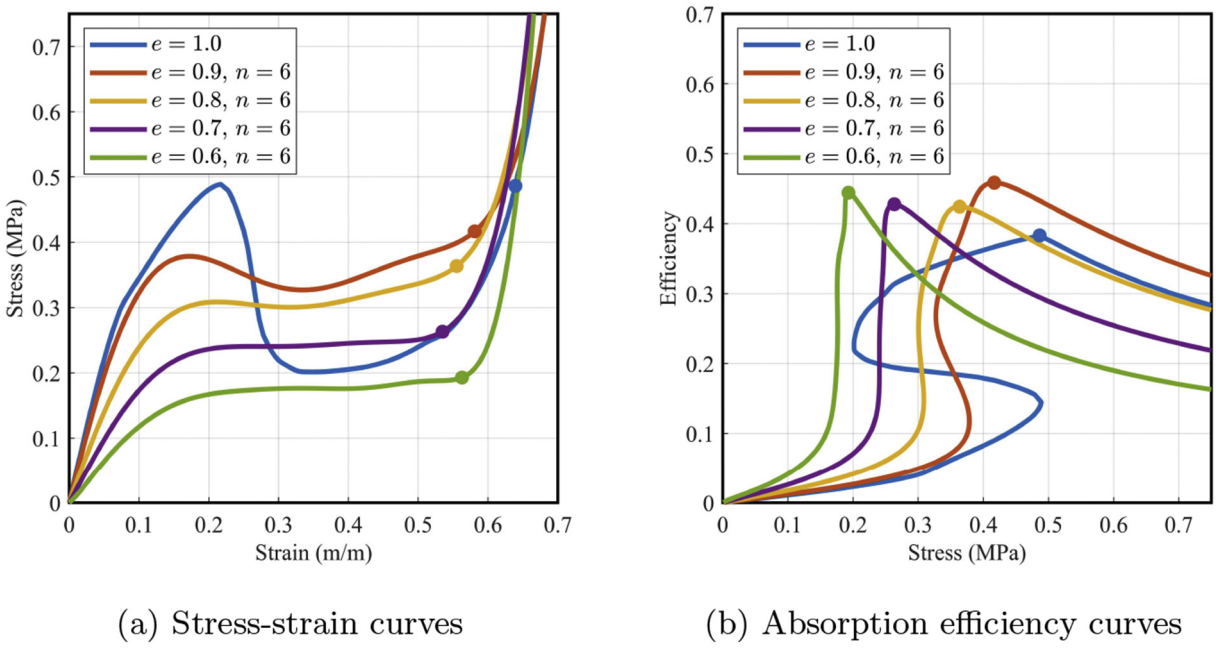

Fig. 4. Experimental compression test results for origami honeycomb with various aspect ratios e. The dots on each curve denote the point of maximum absorption efficiency.

reducing the aspect ratio e will reduce the initial linear slope and peak stress, and lead to a flatter plateau with lower stress value, while increasing the number of folds n will reduce the length of the plateau (reduce the densification strain), leading to more linear responses.

The stress-softening and hysteresis behavior was investigated via cyclic compression loading up to 0.7 strain at 100 mm/min, with 1 minute relaxation between cycles. The results of one such test are shown in Fig. 6 for the $e = 0.7$, $n = 6$ honeycomb. The right and left arrows indicate the loading and unloading phases, while the numbers in parentheses track the specific energy absorbed up to the point of maximum absorption efficiency for each cycle. A 17% reduction in absorbed energy is evident between the first and second compression cycles, however subsequent cycles vary by less than 4%. The TPU material thus undergoes a softening behavior during cyclic loading, with the majority of softening occurring on the first cycle, stabilizing after four cycles. Analogous behavior has been observed in neat TPU [24] and 3D printed TPU honeycombs under in-plane compression [10]. The Ninjaflex honeycombs tested in [10] with relative density 0.22 absorbed 0.028 J/cm^3 with an efficiency of 0.35 on the 5th compression cycle. The origami honeycomb (which recall has relative density 0.21) absorbed 0.089 J/cm^3 with an efficiency of 0.42, improvements of 218% and 20% respectively. The marked improvement in energy absorption highlights the benefits of utilizing the stiffness-to-weight ratio of honeycombs compressed in the out-of-plane direction. When combined with

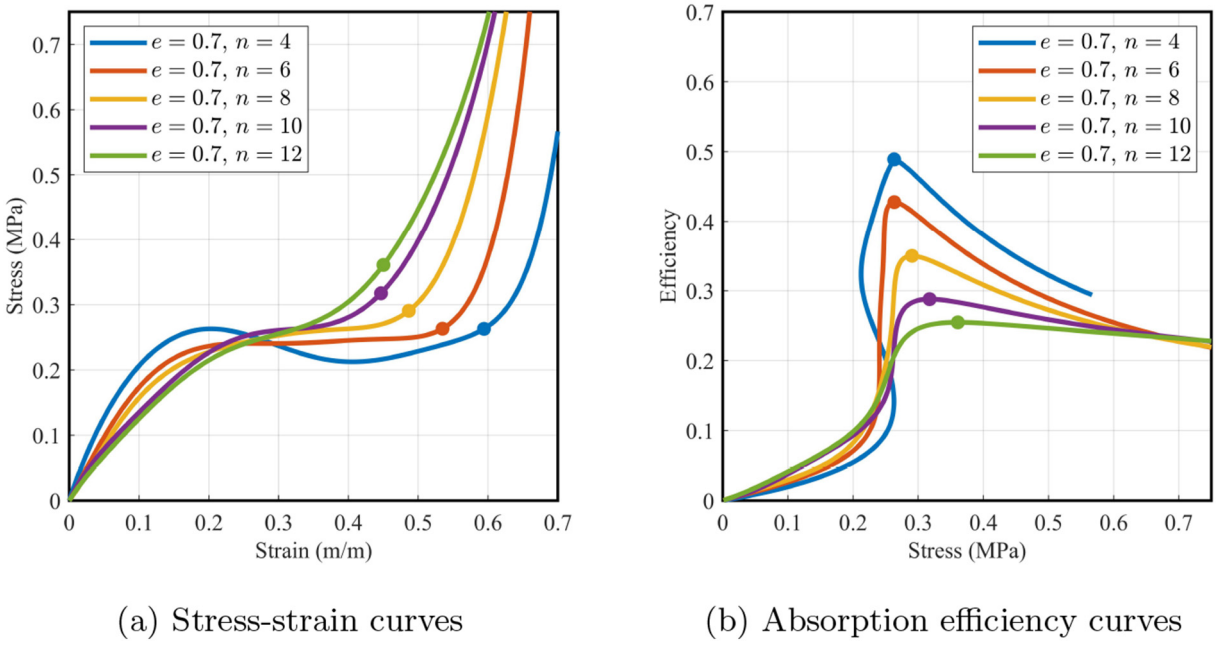

Fig. 5. Experimental compression test results for origami honeycomb with various number of folds n. The dots on each curve denote the point of maximum absorption efficiency.

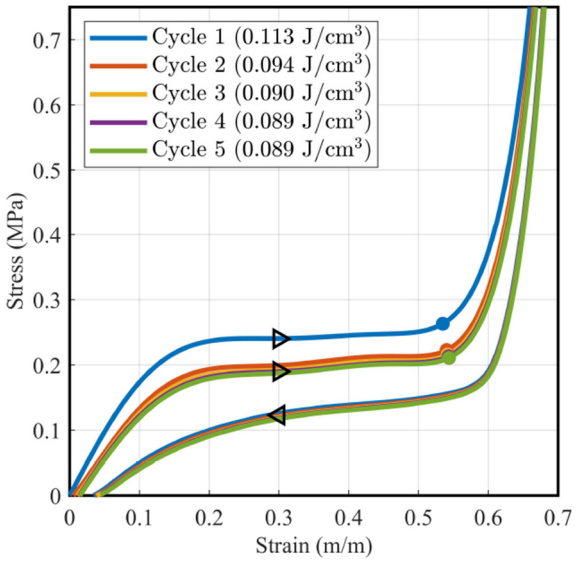

Fig. 6. Cyclic compression loading for the $e = 0.7$, $n = 6$ honeycomb. Right and left arrows denote loading and unloading respectively. Dots on the curves and the numbers in parentheses denote point of maximum absorption efficiency, and specific energy absorbed up to that strain, respectively.

origami folding, high absorption efficiency can be maintained. As demonstrated in [10], the energy absorption can be further increased by utilizing a stiffer TPU material, without sacrificing efficiency. Though not plotted for the sake of clarity, we also tested this specimen after 15 minute, 1 hour and 24 hour relaxation, and each cycle measured a specific energy absorption of 0.094 J/cm^3. This suggests that the large drop observed between the first and second loading cycles has a recovery time longer than 24 h, or could suggest some plastic damage is occurring during the first compression cycle. Evidence of the latter was present in the form of mild discoloration near the origami folds. The stress-softening that occurs on subsequent compression cycles appears to be recoverable.

5. Conclusions

This work documents the incorporation of origami folds into square honeycombs, which were realized using the 3D printed thermoplastic polyurethane, Ninjaflex. The effect of the fold parameters on the honeycomb out-of-plane energy absorption behavior was investigated using both finite element analysis and experimental methods. Increasing the severity of the fold angle was demonstrated to reduce the overall stiffness of the structure, and produce quasi-rectangular absorption profiles. Increasing the number of folds was shown to shorten the width of the stress plateau, and produce quasi-linear absorption profiles. Absorption efficiency parameters as high as 0.49 were measured experimentally, which rival rigid polyurethane foams. Cyclic compression testing demonstrated a moderate stress-softening effect on the first cycle, which lessened for subsequent compressions. Given the versatility of absorption behaviors observed, the structures presented herein hold excellent potential for applications requiring tailored energy absorption profiles.

CRediT authorship contribution statement

Scott Townsend: Conceptualization, Methodology, Software, Investigation, Data curation, Writing - original draft, Writing - review & editing. **Rhosslyn Adams:** Conceptualization, Methodology, Investigation, Writing - review & editing. **Michael Robinson:** Conceptualization, Methodology, Writing - review & editing. **Benjamin Hanna:** Conceptualization, Methodology, Writing - review & editing. **Peter Theobald:** Writing - review & editing, Supervision, Funding acquisition.

Declaration of Competing Interest

The authors declare that they have no known competing financial interests or personal relationships that could have appeared to influence the work reported in this paper.

Acknowledgments

This research was financially-supported by Football Research, Inc. under the Head Health Tech V program.

Data availability

All data supporting this study, including 3D printable STL files, is openly available in the Figshare data repository at https://doi.org/10.6084/m9.figshare.c.5067491.

References

[1] L.J. Gibson, M.F. Ashby, Cellular Solids: Structure and Properties, Cambridge University press, 1999https://doi.org/10.1017/CBO9781139878326.
[2] T. Bitzer, Honeycomb Technology: Materials, Design, Manufacturing, Applications and Testing, Springer Science & Business Media, 1997 https://doi.org/10.1007/978-94-011-5856-5.
[3] T. Wierzbicki, W. Abramowicz, On the crushing mechanics of thin-walled structures, J. Appl. Mech. 50 (4a) (1983) 727–734, https://doi.org/10.1115/1.3167137.
[4] D. Wang, Impact behavior and energy absorption of paper honeycomb sandwich panels, Int. J. Impact Eng. 36 (1) (2009) 110–114, https://doi.org/10.1016/j.ijimpeng.2008.03.002.
[5] D.C. Mackey, C.C. Lachance, P.T. Wang, F. Feldman, A.C. Laing, P.M. Leung, X.J. Hu, S.N. Robinovitch, The flooring for injury prevention (flip) study of compliant flooring for the prevention of fall-related injuries in long-term care: a randomized trial, PLoS Med. 16 (6) (2019), e1002843. https://doi.org/10.1371/journal.pmed.1002843.
[6] O. Duncan, T. Shepherd, C. Moroney, L. Foster, P. Venkatraman, K. Winwood, T. Allen, A. Alderson, Review of auxetic materials for sports applications: expanding options in comfort and protection, Appl. Sci. 8 (6) (2018) 941, https://doi.org/10.3390/app8060941.
[7] P. Zhang, D.J. Arceneaux, A. Khattab, Mechanical properties of 3d printed polycaprolactone honeycomb structure, J. Appl. Polym. Sci. 135 (12) (2018), 46018. https://doi.org/10.1002/app.46018.
[8] Y. Yap, W. Yeong, Shape recovery effect of 3d printed polymeric honeycomb: this paper studies the elastic behaviour of different honeycomb structures produced by polyjet technology, Virtual Phys. Prototyp. 10 (2) (2015) 91–99, https://doi.org/10.1080/17452759.2015.1060350.
[9] J. Yi, M. Boyce, G. Lee, E. Balizer, Large deformation rate-dependent stress–strain behavior of polyurea and polyurethanes, Polymer 47 (1) (2006) 319–329, https://doi.org/10.1016/j.polymer.2005.10.107.
[10] S.R. Bates, I.R. Farrow, R.S. Trask, 3d printed polyurethane honeycombs for repeated tailored energy absorption, Mater. Des. 112 (2016) 172–183, https://doi.org/10.1016/j.matdes.2016.08.062.
[11] S.R. Bates, I.R. Farrow, R.S. Trask, Compressive behaviour of 3d printed thermoplastic polyurethane honeycombs with graded densities, Mater. Des. 162 (2019) 130–142, https://doi.org/10.1016/j.matdes.2018.11.019.
[12] M. Robinson, S. Soe, R. Johnston, R. Adams, B. Hanna, R. Burek, G. McShane, R. Celeghini, M. Alves, P. Theobald, Mechanical characterisation of additively manufactured elastomeric structures for variable strain rate applications, Additive Manuf. 27 (2019) 398–407, https://doi.org/10.1016/j.addma.2019.03.022.
[13] S. Deqiang, Z. Weihong, W. Yanbin, Mean out-of-plane dynamic plateau stresses of hexagonal honeycomb cores under impact loadings, Compos. Struct. 92 (11) (2010) 2609–2621, https://doi.org/10.1016/j.compstruct.2010.03.016.
[14] S. Duan, Y. Tao, H. Lei, W. Wen, J. Liang, D. Fang, Enhanced out-of-plane compressive strength and energy absorption of 3d printed square and hexagonal honeycombs with variable-thickness cell edges, Extreme Mech. Lett. 18 (2018) 9–18, https://doi.org/10.1016/j.eml.2017.09.016.
[15] S. Yin, J. Li, B. Liu, K. Meng, Y. Huan, S.R. Nutt, J. Xu, Honeytubes: hollow lattice truss reinforced honeycombs for crushing protection, Compos. Struct. 160 (2017) 1147–1154, https://doi.org/10.1016/j.compstruct.2016.11.007.
[16] J. Fang, G. Sun, N. Qiu, T. Pang, S. Li, Q. Li, On hierarchical honeycombs under out-of-plane crushing, Int. J. Solids Struct. 135 (2018) 1–13, https://doi.org/10.1016/j.ijsolstr.2017.08.013.
[17] J. Ma, Z. You, Energy absorption of thin-walled square tubes with a prefolded origami pattern–part i: geometry and numerical simulation, J. Appl. Mech. 81 (1) (2014), 011003. https://doi.org/10.1115/1.4024405.

[18] J. Ma, D. Hou, Y. Chen, Z. You, Quasi-static axial crushing of thin-walled tubes with a kite-shape rigid origami pattern: numerical simulation, Thin-Walled Struct. 100 (2016) 38–47, https://doi.org/10.1016/j.tws.2015.11.023.
[19] J. Song, Y. Chen, G. Lu, Axial crushing of thin-walled structures with origami patterns, Thin-Walled Struct. 54 (2012) 65–71, https://doi.org/10.1016/j.tws.2012.02.007.
[20] W. Abramowicz, N. Jones, Dynamic axial crushing of square tubes, Int. J. Impact Eng. 2 (2) (1984) 179–208, https://doi.org/10.1016/0734-743X(84)90005-8.
[21] S. Liang, H. Chen, Investigation on the square cell honeycomb structures under axial loading, Compos. Struct. 72 (4) (2006) 446–454, https://doi.org/10.1016/j.compstruct.2005.01.022.
[22] M. Avalle, G. Belingardi, R. Montanini, Characterization of polymeric structural foams under compressive impact loading by means of energy-absorption diagram, Int. J. Impact Eng. 25 (5) (2001) 455–472, https://doi.org/10.1016/S0734-743X(00)00060-9.
[23] J. Miltz, O. Ramon, Energy absorption characteristics of polymeric foams used as cushioning materials, Polym. Eng. Sci. 30 (2) (1990) 129–133, https://doi.org/10.1002/pen.760300210.
[24] H.J. Qi, M.C. Boyce, Stress–strain behavior of thermoplastic polyurethanes, Mech. Mater. 37 (8) (2005) 817–839, https://doi.org/10.1016/j.mechmat.2004.08.001.